



HAL
open science

Arctic polar vortex during THESEO and THESEO 2000

E. Riviere, Michel Pirre, Gwenaël Berthet, Jean-Baptiste Renard, F G Taupin, Nathalie Huret, Michel Chartier, B Knudsen, F Lefèvre

► To cite this version:

E. Riviere, Michel Pirre, Gwenaël Berthet, Jean-Baptiste Renard, F G Taupin, et al.. Arctic polar vortex during THESEO and THESEO 2000. *Journal of Geophysical Research: Atmospheres*, 2002, 107 (D5), pp.54. 10.1029/2002JD002087 . insu-02879024

HAL Id: insu-02879024

<https://insu.hal.science/insu-02879024>

Submitted on 23 Jun 2020

HAL is a multi-disciplinary open access archive for the deposit and dissemination of scientific research documents, whether they are published or not. The documents may come from teaching and research institutions in France or abroad, or from public or private research centers.

L'archive ouverte pluridisciplinaire **HAL**, est destinée au dépôt et à la diffusion de documents scientifiques de niveau recherche, publiés ou non, émanant des établissements d'enseignement et de recherche français ou étrangers, des laboratoires publics ou privés.

On the interaction between nitrogen and halogen species in the Arctic polar vortex during THESEO and THESEO 2000

E. D. Rivière, M. Pirre, G. Berthet, J.-B. Renard, F. G. Taupin, N. Huret, and M. Chartier

Laboratoire de Physique et Chimie de l'Environnement/CNRS, Université d'Orléans, Orléans, France

B. Knudsen

Danish Meteorological Institute, Copenhagen, Denmark

F. Lefèvre

Service d'Aéronomie, Institut Pierre-Simon Laplace, Paris, France

Received 14 January 2002; revised 18 June 2002; accepted 18 June 2002; published 22 November 2002.

[1] Large disagreements between measured and simulated NO_2 have been observed several times in the Arctic polar vortex. Here we report on the comparison of two sets of nighttime balloonborne measurements of the couple (OCIO, NO_2) with Lagrangian model outputs in order to study the interactions between halogen and nitrogen species. Those measurements were characterized by the simultaneous presence of significant amounts of both species. Large disagreements are observed between modeled and measured NO_2 . Very surprisingly, good agreement can be achieved for OCIO in spite of the supposed strong coupling between these two species. The only simultaneous agreement between model and measurements for both species occurs in the case of denoxified conditions, i.e., when there is no interaction between halogen and nitrogen compounds. Furthermore, agreement for OCIO cannot be obtained if a source for NO_2 is assumed to fit the measurements of this specie. This result shows that some uncertainties still exist in the interaction between nitrogen and halogen species. *INDEX TERMS:* 0340 Atmospheric Composition and Structure: Middle atmosphere—composition and chemistry; 3337 Meteorology and Atmospheric Dynamics: Numerical modeling and data assimilation; 3360 Meteorology and Atmospheric Dynamics: Remote sensing; *KEYWORDS:* OCIO, NO_2 , deactivation, Arctic stratosphere, balloonborne measurement

Citation: Rivière, E. D., M. Pirre, G. Berthet, J.-B. Renard, F. G. Taupin, N. Huret, M. Chartier, B. Knudsen, and F. Lefèvre, On the interaction between nitrogen and halogen species in the Arctic polar vortex during THESEO and THESEO 2000, *J. Geophys. Res.*, 107, 8311, doi:10.1029/2002JD002087, 2002. [printed 108(D5), 2003]

1. Introduction

[2] Inorganic chlorine species (Cl_y) play a key role in polar vortex stratospheric chemistry. Active species (ClO_x) are involved in catalytic cycles that destroy ozone while others, like HCl, ClONO_2 and HOCl, act as potential sources (reservoirs) for these active species. Nitrogen NO_x ($\text{NO} + \text{NO}_2$) also play an important role in the ozone recovery mechanism, in deactivating chlorine in particular at the end of winter. However, if the main mechanisms such as activation, deactivation and denitrification seem well identified, problems appear in the quantification of each process. For example, ozone depletion and chlorine activation are usually underestimated by chemistry transport models (CTM) if recommended rate coefficients are used [i.e., Solomon *et al.*, 2000; van den Broek *et al.*, 2000]. Moreover, a few studies conducted in the polar vortex have reported significantly higher measured NO_2

concentrations than model simulations [Lary *et al.*, 1997; Payan *et al.*, 1999a; Wetzel *et al.*, 1997]. At low altitude in particular, the model simulations lead to a full denoxification of the whole polar vortex while some residual NO_2 concentrations are still measured. In the model, such a full denoxification is necessary to maintain chlorine activation at a sufficient level to deplete ozone. Constraining the models with the measured NO_2 would lead to a significant chlorine deactivation and therefore to a reduction of the simulated ozone depletion increasing the disagreement with measured ozone loss. As a consequence, the simultaneous observation of both residual NO_2 concentration and chlorine activation must mean that something is not understood in the interaction between halogen and nitrogen species. The aim of this paper is to demonstrate such misunderstanding by using simultaneous nighttime profile measurements of OCIO and NO_2 by balloonborne UV-visible spectrometers and simulations using a Lagrangian model.

[3] The use of simultaneous measurements of NO_2 and OCIO is a powerful technique to achieve this goal if we

consider the OCIO chemistry. OCIO is generally assumed to form at sunset by one of the three branches of the reaction between bromine and chlorine oxides:



[4] In very unusual warm conditions the reaction $\text{ClO} + \text{ClO}$ has been reported to be a potential source of OCIO [Pierson *et al.*, 1999].



[5] According to our present knowledge, the production rate of OCIO in both cases is reduced by the following reactions in competition with R1c and R2:



OCIO is therefore sensitive to the actual NO_2 concentration.

[6] The only significant path for OCIO destruction is the rapid photolysis for solar zenith angles (hereafter *sza*), lower than 92° . As a consequence, the OCIO concentration is almost constant during nighttime. In case of chlorine activation, it has been shown that this nighttime concentration is not dependent on the ClO concentration but is almost proportional to the before sunset BrO concentration [Sessler *et al.*, 1995; Schiller and Wahner, 1996].

[7] Measurements of OCIO in the atmosphere were reported for the first time by Solomon *et al.* [1988]. Later, several other ground-based twilight measurements of OCIO were published [Schiller *et al.*, 1990; Kreher *et al.*, 1996; Gil *et al.*, 1996] as well as a more recent study [Sanders *et al.*, 1999]. There are very few profile measurements of OCIO in the stratosphere. The DOAS instrument (profile presented by Payan *et al.* [1999b]) and the SAOZ spectrometer [Pommereau and Piquard, 1994a] at twilight, and AMON [Renard *et al.*, 1997] and SALOMON at night are the only instruments known to us to make such measurements.

[8] Many profile measurements of NO_2 in the stratosphere are reported in the literature but most of them are performed at twilight using the solar occultation technique [Payan *et al.*, 1999a; Pommereau and Piquard, 1994b]. To our knowledge, the only nighttime profile measurements of NO_2 in the stratosphere have been performed by the balloonborne AMON [Renard *et al.*, 1996], SALOMON [Renard *et al.*, 2000], MIPAS [Wetzel *et al.*, 1997] spectrometers, and by the CLAES [Roche *et al.*, 1993] satellite instrument.

[9] Up to now simultaneous measurements of OCIO and NO_2 at night have only been made by the AMON and SALOMON balloonborne instruments. In this paper, we use measurements made by AMON during the THESEO campaign in February 1999 and by SALOMON in January 2000 during the THESEO 2000 campaign. These instruments operate by stellar or lunar occultation. The primary measurements are therefore the slant columns of the species

along the line of sight. The inversion of the vertical profiles assumes horizontal homogeneities of the atmospheric layers over a few hundred kilometer. Both cases have been chosen because this hypothesis is valid at the best. Indeed, measurements are made during the night while species concentrations are not varying as a function of local time. This prevents the inhomogeneities observed in the case of measurements made at twilight. Moreover, in the two cases, all the points of the lines of sight, for star or Moon zenith angles above 90° , are well inside the vortex, at least for altitudes below 30 km. All the profiles are interpreted with the Lagrangian model MiPLaSMO (Microphysical and Photochemical Lagrangian Stratospheric Model of Ozone) [Rivièrè *et al.*, 2000].

2. Instrumentation and Model Description

2.1. Instrumentation

2.1.1. AMON

[10] AMON (French acronym for Absorption par Minoritaires Ozone et NO_x) is a balloonborne UV-visible spectrometer. It is dedicated to nighttime measurements of stratospheric O_3 , NO_2 , NO_3 , OCIO and aerosol extinction. The spectrometer covers continuously the UV-visible spectral domain from 350 to 700 nm. A full description of the instrument, its accuracy, and of the data reduction for NO_2 and OCIO is given by Renard *et al.* [1996, 1997, 1998]. Observations are performed using the stellar occultation method, which consists in analyzing the modifications of the spectrum of a setting star caused by absorbing atmospheric compounds. A reference spectrum is obtained when the light source (i.e., the star) is above the balloon horizon and the balloon is at its highest altitude (float). The transmission spectra are obtained by dividing the observed spectra by the reference spectrum. The slant column densities are retrieved using a least squares fit between the observed transmission spectra and the spectra calculated using the well-known cross sections of the absorbing species. The aerosol contribution in the extinction is the residual in the transmission spectra, after removing the contribution of Rayleigh scattering and of molecular absorption. The vertical profiles of the species and of the aerosol extinction are obtained after inversion using least squares fit method.

2.1.2. SALOMON

[11] SALOMON (French acronym for Spectrométrie d'Absorption Lunaire pour L'Observation des Minoritaires Ozone et NO_x) is a spectrometer which operates continuously in the UV-visible spectral domain.

[12] SALOMON is devoted to the measurement of the same species as AMON, but uses the Moon as a light source. Considering that the moonlight flux is greater than the star flux, SALOMON can detect absorption features of 10^{-4} which is ten times better than that of AMON. However, the vertical resolution is reduced compared to that of AMON because of the large apparent diameter of the Moon (0.5°) which leads to a resolution of 1 to 2 km. For further details, see Renard *et al.* [2000].

2.2. MiPLaSMO

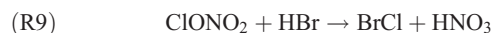
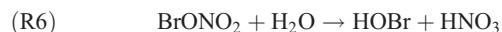
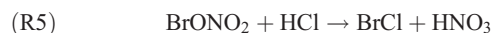
[13] MiPLaSMO has been developed at LPCE (Laboratoire de Physique et Chimie de l'Environnement) to study

in detail the stratospheric ozone chemistry in polar regions. It is composed of a microphysical spectral polar stratospheric cloud (PSC) model first developed at the Danish Meteorological Institute [Larsen *et al.*, 1997], a photochemical model involving 125 reactions and which describes the evolution of 42 species. Simulations are performed along isentropic trajectories calculated off line by a routine developed by Knudsen *et al.* [2001]. This model allows the time evolution of all the species, PSCs and aerosol size distributions, and chemical rate coefficients to be followed along air parcel trajectories. A more detailed description of the model is given by Rivière *et al.* [2000].

[14] Below we present the improvements that have been carried out since the above-mentioned study:

[15] Chemical rate constants and cross sections have been updated according to Sander *et al.* [2000].

[16] Heterogeneous reactions involving bromine species have been included. These reactions are:



[17] Finally the calculations of the photolysis coefficients has been improved by including the TUV (Tropospheric Ultraviolet-Visible) radiation model developed by Madronich and Flocke [1999] at NCAR. This allows calculation of actinic fluxes taking into account realistic O₂ and ozone column densities and reflectivities along the trajectories. Here column densities are computed using satellite ozone measurements. Before a simulation is performed, we check for any satellite measurement along the trajectory that would correspond both in time and location to the one of the air parcel within a reasonable distance. This distance may vary as a function of location of both air parcel and measurements within the vortex. Ozone and O₂ columns are updated along the trajectory each time the air parcel coincides with a satellite measurement location. The reflectivity data used in the model are also taken from satellite measurements.

3. Case of 23 January 2000

3.1. Measurement Context

[18] The SALOMON flight of January 2000 occurred at Kiruna (67.9°N/22.1°E), Sweden, as part of the THESEO 2000 campaign. The measurement time was around 1700 UT and spectra were collected during moonrise. The altitude float was 26.5 ± 1.2 km. Four points of measurements could be retrieved between 13.8 and 18.2 km (124 to 59 hPa, respectively). The balloon and the optical path during the measurements were well inside the polar vortex as shown in Figure 1. Low temperatures prevailing during this period led to a high chlorine activation and to a substantial denoxifi-

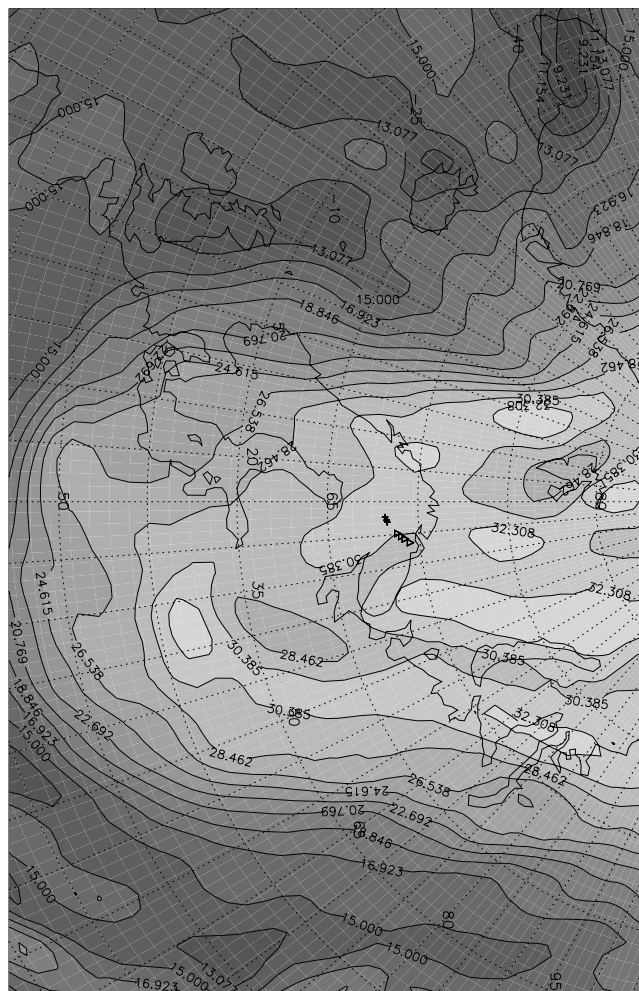


Figure 1. Arctic polar vortex on 23 January 2000 at 18 UT at 433 K (18.2 km). PV contours are drawn. PV values increase from dark to white colors. Also shown are the intersection points of a few lines of sights from the SALOMON gondola, located at 26 km, with the 433 K level. Crosses indicate the entry point while triangles indicate the exit points.

cation of the whole vortex, as indicated by 3-D simulations with the REPROBUS CTM.

3.2. Comparison Between Model and Measurements

3.2.1. Initialization of MiPLaSMO

[19] Ten day backtrajectories are used for the simulations. The endpoint of each trajectory corresponds to the tangent point of the optical path, which is the most representative point of a considered atmospheric layer along the optical path. The chemical species initial values are taken from the REPROBUS chemical transport model [Lefèvre *et al.*, 1998] at the beginning of each trajectory. Measurements of the University of Wyoming Optical Particle Counter (UW-OPC) [Deshler *et al.*, 1993] on 19 January 2000 available on the NILU database, are used for aerosol initialization in the model. Ozone and O₂ columns used for the simulations are taken for the POAM3 measurements of 17, 19, 20, and 23 January 2000. Reflectivity data used were measured by the TOMS instrument onboard the Earth Probe spacecraft,

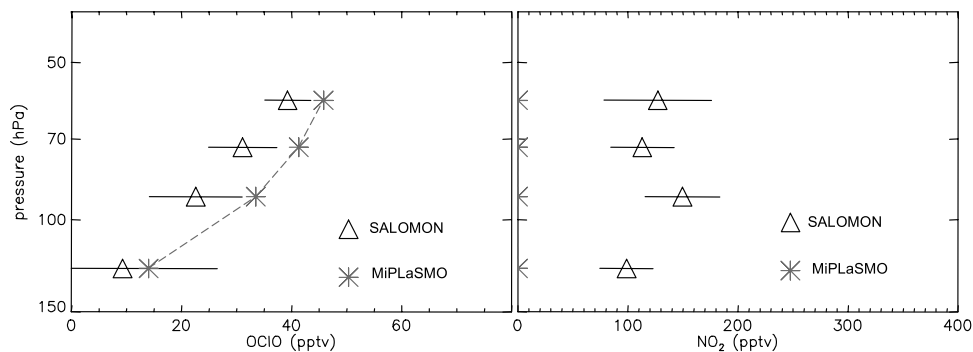


Figure 2. Measured and simulated profiles of OCIO (left panel) and NO_2 (right panel) on 23 January 2000, over Kiruna. Measurements by SALOMON are shown with triangles. MiPLaSMO simulations are shown in gray dotted line and stars.

given once per day. Thus reflectivity data are updated everyday along the trajectory.

3.2.2. Results

[20] Figure 2 shows the SALOMON measurements of OCIO and NO_2 and the corresponding simulations by MiPLaSMO. The NO_2 measurements are characterized by significantly nonzero mixing ratios around 100–150 pptv.

[21] Concerning the OCIO profile, a linear increase in measured OCIO mixing ratio from 9 to 39 pptv is observed as a function of altitude. This behavior is well reproduced by the model and furthermore, even if slightly overestimated for the three higher levels (90, 73, and 59 hPa), the OCIO mixing ratios computed are in rather good agreement with the measurements at each level considered. A detailed analysis of the model results confirms that in that case, $\text{BrO} + \text{ClO}$ (R1c) is the only significant way of forming OCIO. The OCIO production via the $\text{ClO} + \text{ClO}$ (R2) reaction only represents 0.2 pptv in the low temperature conditions (193–200 K) that prevailed here. In particular conditions, this last reaction has been shown to be significant by *Pierson et al.* [1999] where a 225 K temperature was observed during the formation of OCIO. As the constant rate for reaction R2 is faster in warm stratospheric temperature conditions, the R2 impact on OCIO formation can have been significant for the *Pierson et al.* [1999] study. Our conditions are very different because temperatures are much lower when OCIO forms and reaction R1c is then predominant.

[22] In agreement with 3-D simulations, NO_2 mixing ratios computed by MiPLaSMO are very low (lower than 1 pptv) at each level. To explain this behavior, the sza evolution during the 10 day backtrajectory at the 412 K level (73 hPa at the end of the trajectory) is plotted in Figure 3. It shows that during the 10 days prior to the measurements, the sun is always below the horizon ($\text{sza} > 90^\circ$). Furthermore, due to the low temperatures prevailing in January in the vortex, chlorine was activated since the beginning of the simulations leading to a full denoxification. The weak solar fluxes encountered along the trajectory reduce dramatically the possibility of NO_2 formation from HNO_3 photodissociation and oxidation by OH.

4. Case of 12 February 1999

4.1. Measurement Context

[23] The AMON flight of 12 February 1999 occurred at Kiruna around 0000 UT during the THESEO campaign.

Measurements were performed within the polar vortex during the setting of the star Alnilam (ϵ Orionis). This star is the source of an important flux in the UV domain, which allows measurements of OCIO. The float altitude was 29 km and profiles were retrieved from 19 to 29 km. Similarly to the January 2000 case, both the balloon location and the optical paths were well inside the vortex. Temperatures were most of the time above the temperature of saturation nitric acid with respect to NAT, T_{NAT} , leading only to a small chlorine activation.

4.2. Comparison Between Model and Measurements

4.2.1. Initialization of MiPLaSMO

4.2.1.1. Temperature Correction in the Trajectories

[24] 16 day backtrajectories were computed using ECMWF analyses. The end point of the trajectories was chosen at the location of the measurement (tangent point) at 24 hPa. The location of the other levels of measurements is less than 100 km away from this point, which should be a negligible difference in the light of the potentially large errors that may occur in trajectory calculations [*Knudsen et al.*, 2001]. This trajectory end is within the vortex at each level of the profile. During the winter, discrepancies were

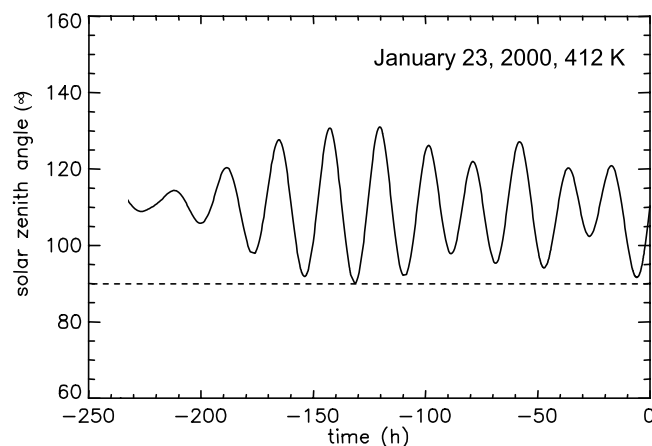


Figure 3. Solar zenith angle (sza) evolution at the 412 K level during the 10 day backtrajectory arriving at Kiruna on 23 January 2000. A dotted line at 90° is added to separate nighttime ($\text{sza} > 90^\circ$) from daytime ($\text{sza} < 90^\circ$). Time 0 h corresponds to the time and location of the measurement.

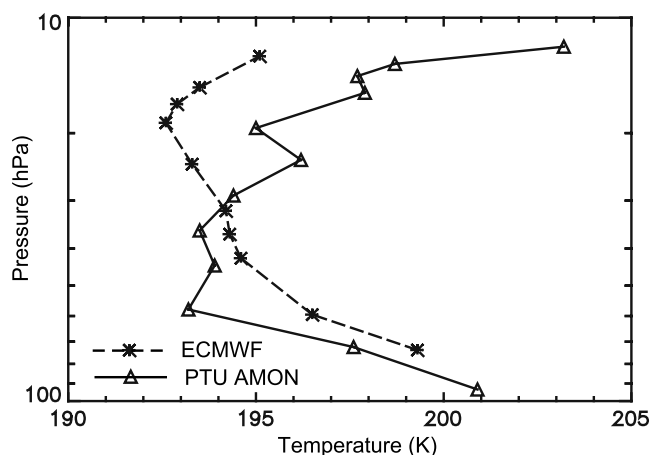


Figure 4. Temperature profile at the measurement location on 12 February 1999. Comparison between temperature from the AMON PTU sonde (solid line and triangles) and from ECMWF analysis (dotted line).

observed between the ECMWF temperatures and the measurements [McNally *et al.*, 1999]. Figure 4 shows the temperatures measured by AMON (T_{AMON}) and the temperatures at the end of the trajectory computed from ECMWF analyses (T_{ECMWF}). ECMWF temperatures are too warm in the lowest levels and are too cold in the highest levels. Reasonable agreement is found from 60 to 30 hPa where differences do not exceed 2 K, but above 30 hPa, differences are more than 3 K, reaching 5 K at 12 hPa. Thus corrections in temperature are needed. In order to use trajectories thermodynamically compatible with the AMON measurements, we have prescribed a $\Delta T = T_{\text{AMON}} - T_{\text{ECMWF}}$ shift of the temperature all along the trajectory for each level.

4.2.1.2. Chemical Species

[25] We have used measurements of ClONO_2 , HNO_3 , NO_2 , HO_2NO_2 and N_2O_5 , from the MIPAS-B instrument [Wetzel *et al.*, 1997] performed from Kiruna on 27 January 1999 at 0558 UT, which give a good indication of total NO_y and the partitioning within this family. Fortunately, the location of the measurements is within a reasonable distance of the starting point of the 16 day backtrajectory in the lowest level (60 hPa). For higher levels, the location of the MIPAS measurements does not correspond to the starting points of the backtrajectories but both are located in air parcels with comparable potential vorticity. Total amount of other main families (Br_y , Cl_y , HO_y , etc. . .) were initialized using REPROBUS chemical transport model outputs on 12 February 1999 over Kiruna. Br_y was initialized as BrCl and Cl_y was initialized as ClONO_2 and HCl using the relation $\text{Cl}_y(\text{REPROBUS}) = \text{ClONO}_2(\text{MIPAS}) + \text{HCl}$. This choice is justified by the fact that the trajectories used are 16 days long, and computed results are not very dependent on the initial partitioning within each family.

4.2.1.3. Aerosols

[26] The aerosol extinction retrieved in this flight of AMON allows an estimation of the surface densities of aerosols (Berthet *et al.*, Optical and physical properties of stratospheric aerosols from balloon measurements in the

visible and the near-infrared domain, 1, Analysis of extinction spectra from the AMON and SALOMON instruments, submitted to *Applied Optics*, 2002, hereinafter referred to as Berthet *et al.*, submitted manuscript, 2002). For this flight, the signal/noise ratio in the extinction limited the aerosol surface retrieval to 3 pressure levels (60, 32 and 19 hPa). For other levels, aerosol surface densities were interpolated between 60 hPa and 19 hPa and extrapolated above 19 hPa using typical surfaces at that level from other AMON and SALOMON flights aerosols (Berthet *et al.*, submitted manuscript, 2002). Then aerosol surfaces at the beginning of the trajectories were chosen in order to correspond to the aerosol surfaces from AMON at the end of the trajectory.

4.2.1.4. O_3 and O_2 Columns and Reflectivity

[27] Ozone and O_2 columns used for the simulations are taken from the POAM3 measurements of 31 January 2000 and 11 February 2000. Reflectivity data are taken from TOMS/Earth Probe measurements.

4.2.2. Results

[28] AMON measurements of OCIO (left panel) and NO_2 (right panel) and corresponding MiPLaSMO outputs are shown in Figure 5. Two sets of simulations are reported in this plot: the “medium aerosol” case is obtained with the mean surface densities estimated by AMON. The “small aerosol” case uses the smallest surface densities allowed by the AMON aerosol retrieval uncertainties. Differences between the two surface densities can reach a maximum of 50%. The log scale has been chosen for the NO_2 panel in order to identify differences between measurements and simulations in the lower part of the profile.

[29] Considering the measurements themselves, the NO_2 profile is characterized by a complete denoxification up to 45 hPa (37 hPa if we account for uncertainties in the measurement that reach 0 pptv for this level) and mixing ratios that reach about 4 ppbv at 10 hPa. The denoxification is well reproduced by MiPLaSMO in the lowermost stratosphere. At higher levels, the calculated NO_2 increases with altitude as observed by AMON, but is considerably underestimated. The discrepancy decreases, in relative, with altitude. Aerosol surface densities have little influence in reducing the discrepancies.

[30] The OCIO profile shows mixing ratio around 65 pptv between 57 and 33 hPa, a slight decrease up to 20 hPa, a peak at 15 hPa and a strong decrease above to 25 pptv. At the lowest levels (i.e., from 60 to 37 hPa), the model results are in relatively good agreement with the measurements considering the error bars. In that altitude region both NO_2 and OCIO seem to be well reproduced by the model. Overall a relatively good agreement is obtained in the case of the smallest aerosol size distribution, even if the model slightly overestimates the OCIO formation from 32 to 19 hPa. In the case of the “medium aerosol” distribution, the model significantly overestimates the AMON profile between the same range of pressure: at 19 hPa, a maximum of 89 pptv is reported by MiPLaSMO while the measurement is about 55 pptv.

[31] NO_2 shows about a 25% increase between 30 and 19 hPa when the “small aerosol” distribution is used: the chlorine activation is less important, and less NO_2 is consumed to deactivate chlorine. At the same time, the computed OCIO shows about a 25% decrease: the enhanced

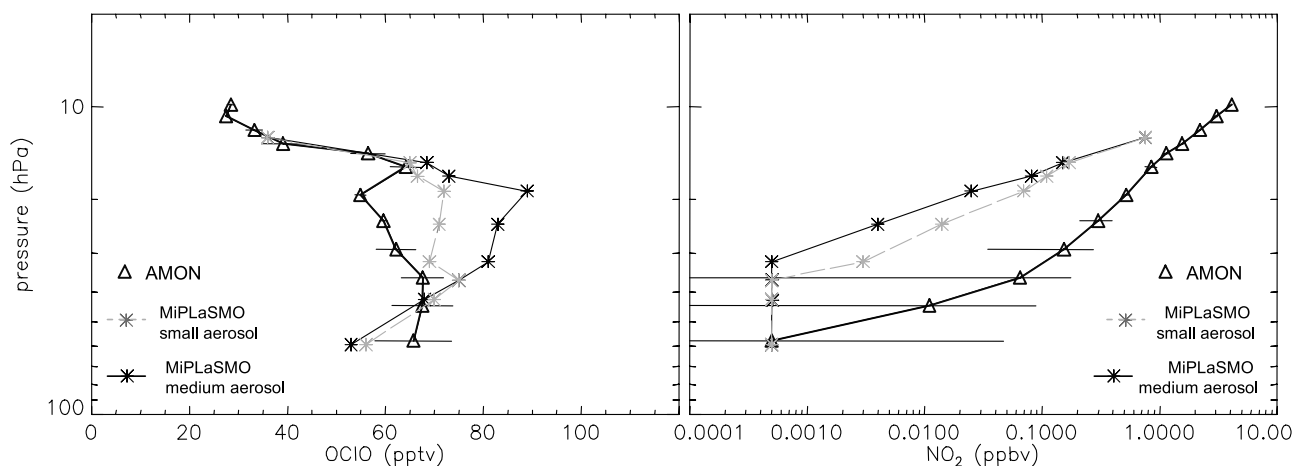


Figure 5. Measured and simulated profiles of OCIO (left panel) and NO_2 (right panel) on 12 February 1999, 0000 UT, over Kiruna. Measurements by AMON are shown by the black line and triangles. MiPLaSMO simulations are shown by the gray dotted line and asterisks in the case of the smaller aerosol size allowed by AMON extinction and by the thin black line and asterisks in the case of medium size aerosols (see text for details). NO_2 values lower than 1 pptv have been set to 0.5 pptv to be visible on the log-scale plot.

NO_2 implies more interaction with BrO, limiting the availability of bromine oxide for OCIO formation.

[32] As on 23 January 2000, there is a substantial underestimation of the computed NO_2 . Interestingly, this disagreement contrasts with the relatively good agreement obtained between the measured and computed OCIO, which is yet a specie very sensitive to the absolute amount of NO_2 .

5. Investigation on the Disagreement Observed

[33] The large disagreement observed between the measured and computed NO_2 has already been observed in the polar vortex [Lary *et al.*, 1997; Payan *et al.*, 1999a; Wetzel *et al.*, 1997; Payan *et al.*, 1999b]. Several hypotheses are investigated in this section.

5.1. Bias in the Inversion Method of the Measurement

[34] The primary measurements of SALOMON and AMON are slant column densities, so one could expect that, OCIO and NO_2 are actually present in the same slant columns but not at the same altitude. For example, in the particular case of 23 January 2000, this means that the retrieved nonzero values of the NO_2 mixing ratio in the range of 13–18 km could actually be a signature of the large mixing ratio simulated above this altitude range as shown in Figure 6a.

[35] This assumption is not possible if, as expected in the retrieval, the layers are horizontally homogeneous. In that case indeed the slant column densities must decrease slightly as the Moon elevation decreases because, the path length of the line of sights in each layer then decreases. As shown in Figure 6b, the slant column densities are actually increasing. Assuming the horizontal homogeneity hypotheses would mean, therefore, that NO_2 mixing ratios have nonzero values in the range of 13–18 km.

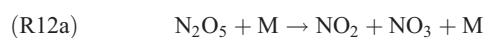
[36] As shown in Figure 6a, this horizontal homogeneity is in fact not strictly true but full 3-D calculations of the slant columns using outputs of the 3-D CTM Reprubus show (Figure 6b) that the simulated slant column densities

nevertheless slightly decrease as Moon elevation decreases despite the horizontal inhomogeneity. Consequently the increasing measured slant column densities as Moon elevation decreases prove definitely that NO_2 mixing ratio have nonzero values in the range of 13–18 km.

[37] The same 3-D calculations have been made for the OCIO column densities. Figure 7a shows that the OCIO mixing ratio is also not strictly horizontally homogeneous. Figure 7b shows that the simulated slant column densities are slightly above the measured ones. This is consistent with the slightly larger OCIO mixing ratio computed with MiPLaSMO (Figure 2). Slant column densities computed assuming zero values for the OCIO mixing ratio below 18 km are also shown in Figure 7b. The very small computed values compared with the measurements show that relatively large OCIO mixing ratio are actually present below this altitude. It is therefore possible to conclude that nonzero values of OCIO and NO_2 mixing ratio are simultaneously measured in the range of 13–18 km.

5.2. Reaction Rate Uncertainties on the NO_2 Budget

[38] Before involving a possible missing source of NO_2 in our present knowledge of the chemistry, the influence of reaction rate uncertainty on the discrepancies previously observed has to be checked. Reactions which could be of prime importance in the NO_2 budget are:



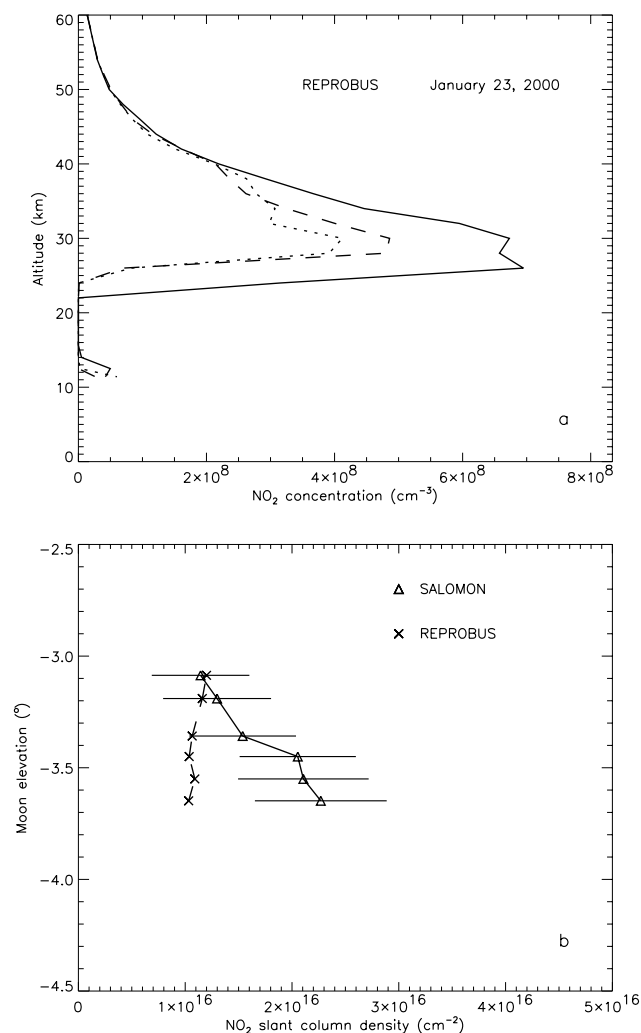


Figure 6. (a) NO₂ vertical profiles computed by the 3-D CTM Reprobis at locations 67 N, 24 E (full line), 70 N, 35 E (dotted line) and 71 N, 38 E (dashed line) on 23 January 2000 at 1700 UT. The balloon altitude is approximately 27 km. The location 67 N, 24 E is the mean of the locations of the entry point of the line of sights for Moon elevation between -3° and -3.7° at 25 km. The location 70 N, 35 E is the mean of the location of the exit points at level between 25 and 35 km for Moon elevation -3° . The location 71 N, 38 E is the mean of the locations of the exit points at levels between 25 and 35 km for Moon elevation -3.7° . The three profiles show that the horizontal homogeneity hypothesis is not strictly true along the lines of sights. (b) Measured slant columns densities as a function of Moon elevation (triangle with error bars and full line) and computed slant column densities using Reprobis simulations and a 3-D geometry (crosses and dashed line).



[39] A sensitivity study has been performed using the most favorable rate constants for high NO₂ mixing ratios for reactions R3 and R10 to R16 within the uncertainties of the reaction rate given by *Sander et al.* [2000] or *DeMore et al.* [1997]. In the case of photolysis reactions (R10, R14 and R16), the uncertainties in the cross sections have been simulated by increasing the photodissociation rates by a factor of two all along the trajectory. The results are plotted in Figure 8 in the case of the smallest aerosol surface distribution.

[40] It appears that no significant change is observed for NO₂ except at 12 hPa where the increased HNO₃ photolysis (R10) becomes important for this trajectory. The relative improvement, at about 30% between both simulations is, however almost not dependent on the altitude. The change in the rate constants also involves a significant decrease in OCIO compared to the case discussed in section 4.2.3 (also shown in Figure 8). This feature is easily understood by considering reaction R4. The small

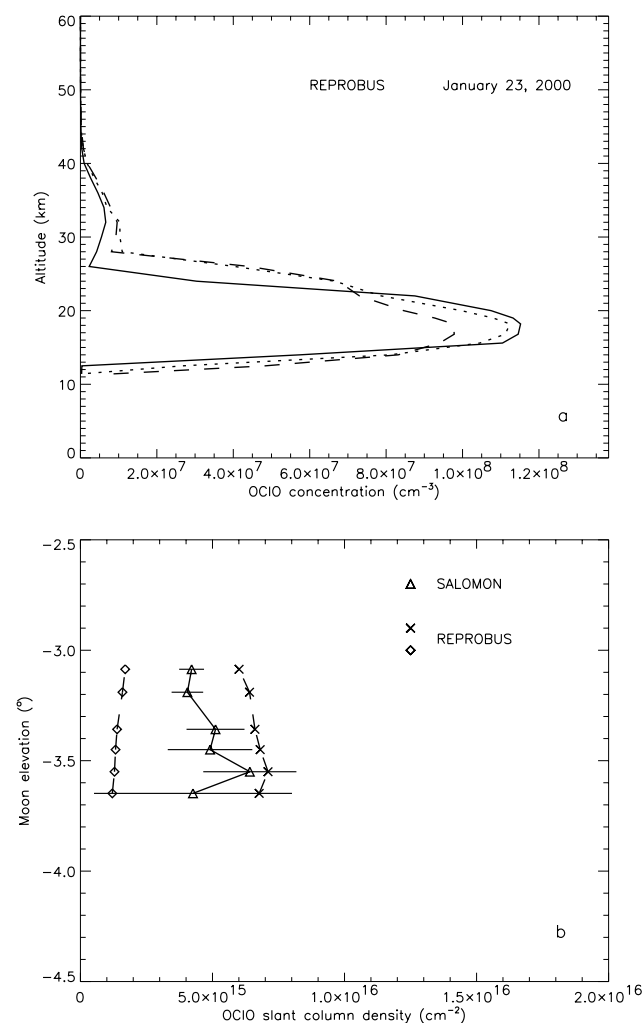


Figure 7. (a) Same as Figure 6a for OCIO. (b) Same as Figure 6b for OCIO. Also shown the slant columns densities computed using Reprobis simulations and a 3-D geometry if OCIO concentration is arbitrarily fixed to zero below 18 km (diamond and dashed line).

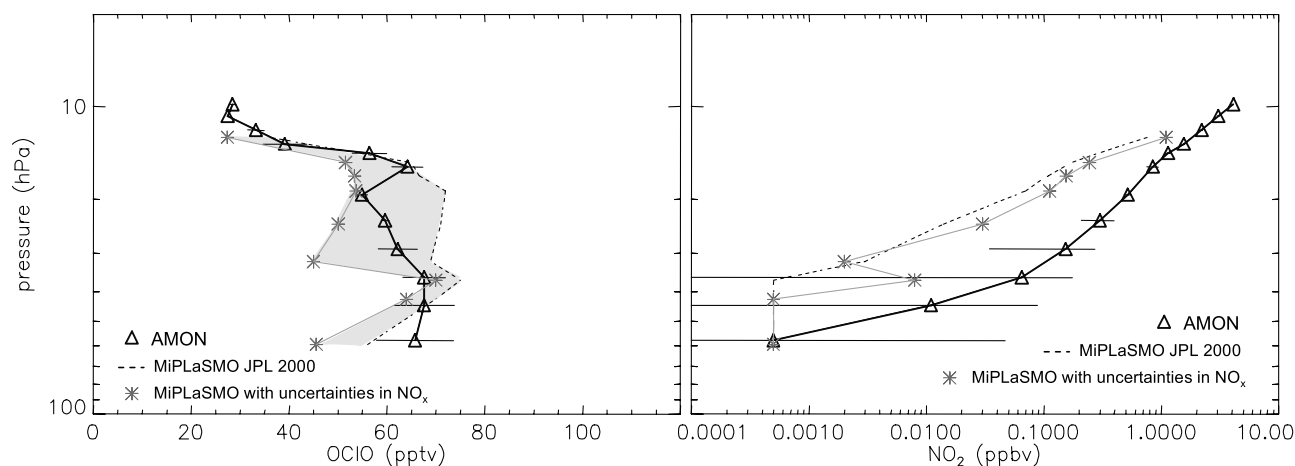


Figure 8. As for Figure 5, except here, MiPLaSMO simulations correspond to the case of the most favorable rate constants for production of NO_2 allowed by uncertainties in reactions R3 and R10 to R16 (gray solid line and asterisks labeled “MiPLaSMO with uncertainties in NO_x ”). Simulations according to JPL 2000 chemistry previously shown in Figure 5 (labeled “MiPLaSMO JPL 2000”) are also shown by the black dotted line. See section 5.2 for details. The domain between the two simulated profiles is shaded gray.

increase of NO_2 consumes BrO which cannot react with ClO to form OCIO. As the concentration of BrO is smaller than the one of ClO, bromine oxide is determining the amount of OCIO production.

[41] In Figure 8, the OCIO measurements are included in the gray domain delimited by the simulated case favorable to a higher NO_2 amount, and the simulated case presented in section 4. This implies that the measured profile of OCIO can be reproduced by MiPLaSMO considering the production of OCIO by R1c, and accounting for uncertainties in the NO_x chemical rates. Such an agreement in OCIO modeling is nevertheless paradoxical, considering the large dependence of OCIO to NO_2 and the simultaneous underestimation in the computed nitrogen dioxide.

[42] It appears that the published uncertainties in reaction rates are not sufficient to explain quantitatively the discrepancies observed between our model calculations and our measurements of nitrogen dioxide. We next consider a missing source of NO_2 in the stratospheric chemistry.

5.3. Renoxification From HNO_3 : A Possible Source of NO_2

[43] Simulations have been carried out with an additional source of NO_2 from HNO_3 , the major reservoir for NO_x species. This source is simulated using the reaction



as of Lary *et al.* [1997], where a source of NO_2 from a heterogeneous reaction of HNO_3 on soot appears to be a possible explanation of the AMON measurements of 1995 in the polar vortex. Recent laboratory works have shown that soot may not be active in the stratosphere [e.g., Saathoff *et al.*, 2001]. Nevertheless, the possibility that soots become active due to aging and changes in their nature has not been explored yet. Preliminary studies suggest that aged soots might be more hydrophilic, and therefore more reactive (J. C. Petit, Laboratoire de

Combustion et des Systèmes Réactifs/CNRS, Orléans, France, personal communication, 2000). However, we do not speculate here on the possible nature of the source of NO_2 . Our aim is to check the impact of an unknown source of NO_2 on the halogen chemistry via the response of the couple [OCIO , NO_2]. Note that the balanced reaction



is not suitable for the simultaneous agreement of NO_2 and OCIO since, as we have tested, enhanced OH radicals transform a large amount of active bromine into HOBr, and thus decrease the OCIO production.

5.3.1. 12 February 1999

[44] The constant rate chosen for reaction R17a is set to $9.7 \cdot 10^{-8} \text{ s}^{-1}$ for all pressure levels. This value has the same order of magnitude as the constant deduced from γ and soot surface area given by Lary *et al.* [1997]. However, it is a slower rate in the present case in order to obtain simulation results comparable with the measurements. Results are presented in Figure 9, using the lowest aerosol size distributions allowed by AMON measurements. Major improvements are obtained for NO_2 : the simulations agree well with the measurements between 60 and 19 hPa and are only slightly underestimated above. However, the model OCIO profile collapses at almost every level compared to the case presented in Figure 6, with minimum values six times lower than the measurements. As in section 5.2, the enhanced amount of NO_2 makes reaction R4 more efficient. BrO is destroyed faster and limits the OCIO production.

5.3.2. 23 January 2000

[45] Similar simulations were performed for the 23 January 2000 case study. A constant rate twice as fast as in the case of February 1999 is needed for reaction R17a to give a calculated NO_2 value in reasonable agreement with the measurements (Figure 10). In the case of a

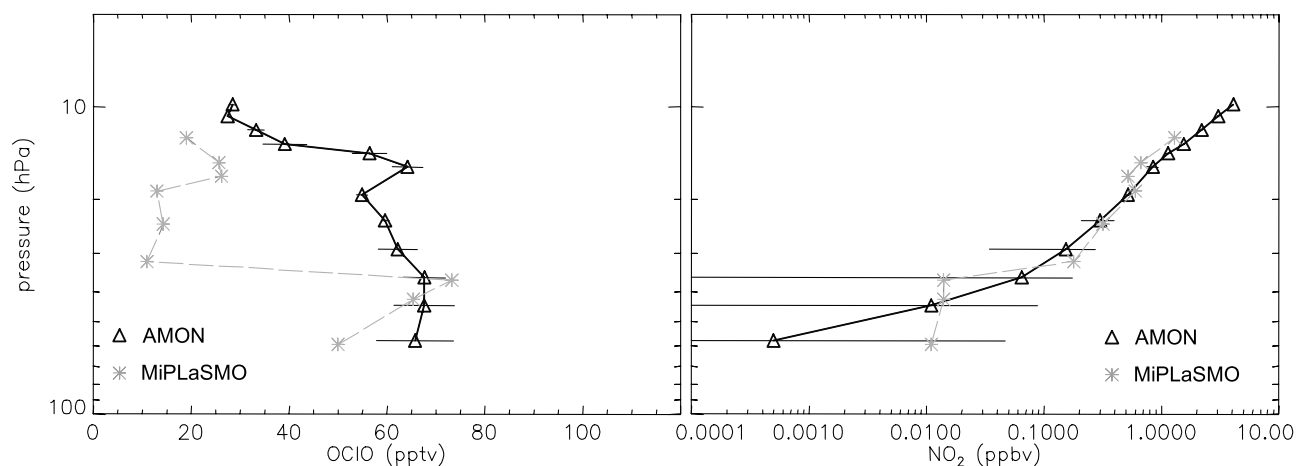


Figure 9. As for Figure 5, except here, MiPLaSMO simulations correspond to the case where a reaction $\text{HNO}_3 \rightarrow \text{NO}_2$ was added to simulate an unknown source of NO_2 . Corresponding simulations of OCIO are shown in the left panel.

heterogeneous source of NO_2 , this increase in the rate constant could be justified by a larger surface area of particles at low altitude. However, as in the case of 12 February 1999, the corresponding computed OCIO concentration is grossly underestimated, with values below 2.5 pptv, except at 412 K (73 hPa) where 27.3 pptv of OCIO are obtained. The computed NO_2 is indeed very small at this level (7.4 pptv).

[46] Clearly, the discrepancies between model and measurements cannot be explained by considering only a “missing” source of NO_2 from HNO_3 , since it would also imply an unrealistically low amount of OCIO in the model. Sensitivity tests have also shown that this source reduces too much chlorine activation and ozone depletion as a comparison with simulations without R17a.

[47] However, the uncertainties in OCIO production have not been taken into account in the above-mentioned simulations. As in section 5.2, simulations were made using the most favorable constant rates to OCIO production and

adding the NO_2 source in the model. Reactions to be taken into account are



[48] Once again, in the case of photodissociation reactions (R18, R19 and R20), the uncertainties have been simulated by increasing the photodissociation rates by a factor of two all along the trajectory. For the 560 K level (33 hPa) simulation case of 12 February 1999, the final mixing ratio of NO_2 is 26 pptv, which is in agreement with the measurements, and OCIO mixing ratio is 29 pptv while 65 pptv were measured. Thus both species cannot be reproduced simulta-

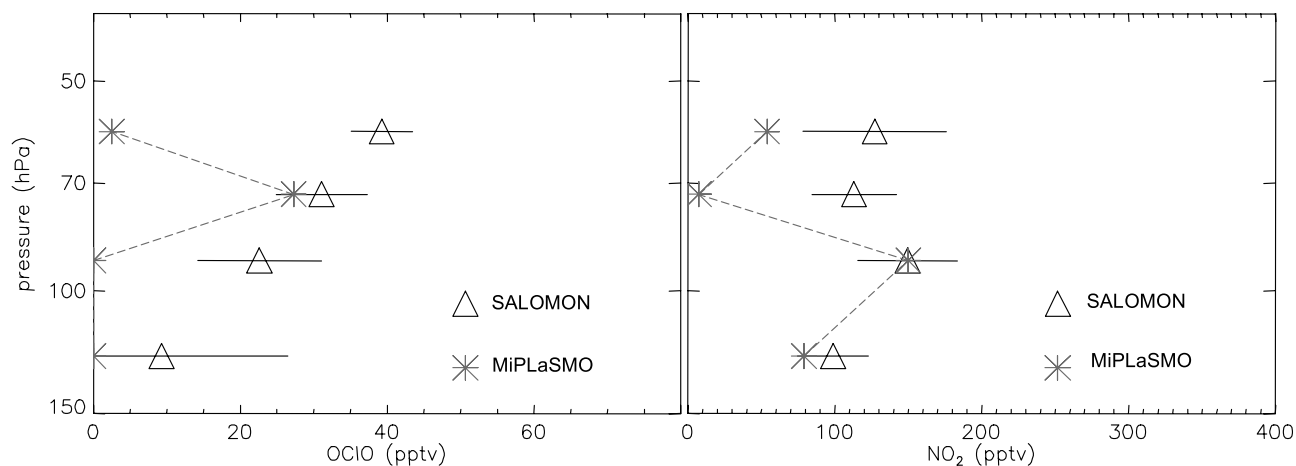


Figure 10. As for Figure 2, except here, MiPLaSMO simulations correspond to the case where a reaction $\text{HNO}_3 \rightarrow \text{NO}_2$ was added to simulate an unknown source of NO_2 . Corresponding simulations of OCIO are shown in the left panel.

nously even if the published uncertainties in OCIO production are taken into account. Sensitivity tests have also been performed concerning the total inorganic bromine. They show that even an unrealistic loading of 35 pptv of Br_y (instead of 20 pptv in the base case) would lead to a underestimated mixing ratio of 19.2 pptv of OCIO when the source of NO₂ is included in the calculations.

6. Discussion

[49] Our results show that it is impossible to reach a simultaneous agreement between our model and measurements of NO₂ and OCIO, given our present knowledge of the interaction between nitrogen and halogen species. It is generally accepted that OCIO is formed by the reaction of ClO with BrO. Its mixing ratio at night is nevertheless mainly dependent on the BrO mixing ratio at sunset. In the model, this BrO mixing ratio is largely reduced in the presence of even small amounts of NO₂. Our measurements and our modeling results show that the efficiency of NO₂ in depleting BrO could be not so large. This means that the rate constant for this reaction could be lower than assumed. Alternatively, the BrONO₂ lifetime might be shorter than expected. After *Orlando and Tyndall* [1996], the thermal decomposition of BrONO₂ is negligible at stratospheric temperatures. The only way around this would therefore be a less stable isomer, formed by the reaction of BrO and NO₂ at low temperature, as it has been found for the reaction OH + NO₂ [Hipler *et al.*, 2001]. With this speculative hypothesis, and if the equilibrium constant between this isomer and BrO is sufficiently in favor of BrO, calculations show that it is possible to reach a simultaneous agreement between measured and simulated BrO and NO₂ for the case of February 1999 but not for the case of January 2000, when a source for NO₂ is assumed. In both cases ClO is decreased by a large amount due to reaction R3. In the first case the mixing ratio of ClO is still sufficiently high to form OCIO, but not in the second case. This means that ClO also is probably too much depleted in the model by its reaction with NO₂.

7. Conclusion and Future Aims

[50] This paper focuses on the interaction between nitrogen and halogen species in the polar vortex. We have used simultaneous nighttime measurements of OCIO and NO₂ that have been compared to model simulations. It has been shown that the model is able to reproduce OCIO rather well in the lower part of the profiles (below 21 km). The production of OCIO by the ClO + ClO reaction does not seem to have a significant impact in this part of the cold polar stratosphere.

[51] NO₂ is underestimated by the model at all levels except when a complete denoxification was observed, on 12 February 1999, below 37 hPa, accounting for uncertainties in the measurements. The uncertainties in reaction rates cannot explain this discrepancy between the model and the measurements, which appears to be in line with results obtained in previous studies [Lary *et al.*, 1997; Wetzel *et al.*, 1997].

[52] A possible missing source of NO₂ and its influence on halogen species has been tested. An additional source of NO₂ from HNO₃ could lead to a reasonable agreement with

the observed NO₂, but its negative impact on OCIO, rules out this simple hypothesis. This source would also reduce the ozone destruction in the model.

[53] Our results show that something is not understood in the interaction between nitrogen and halogen species. To better understand this problem, new simultaneous measurements of nitrogen and halogen species, or the re-analysis of previous measurements are needed to document this issue. Laboratory measurements of the products of the reactions BrO + NO₂ and ClO + NO₂ at low temperature would also be of prime importance. In addition, the measurement of BrONO₂ in the stratosphere would be particularly helpful for understanding the bromine chemistry.

[54] **Acknowledgments.** We thank the CNES (French Center for Space Studies) launch team at Kiruna. We are grateful to Niels Larsen for providing the PSC model, to the POAM3 team for making their data available and to NASA Goddard Space Flight Center for the Earth Probe/TOMS reflectivity data. We do not forget S. Madronich at NCAR for providing the TUV model, Terry Deshler (University of Wyoming) for his aerosol data and Hermann Oelhaf (Institut für Meteorologie und Klimaforschung in Karlsruhe) for providing MIPAS-B measurements. The AMON and SALOMON instruments were funded by CNES. Flights and modeling calculations were supported by French CNRS/PNCA program, by CNES and by European contracts ENV4-CT97-0524 HALOMAX and EVK2-CT-1999-00047 EUROSOLVE.

References

- DeMore, W. B., S. P. Sander, D. M. Golden, R. F. Hampson, M. J. Kurylo, C. J. Howard, A. R. Ravishankara, C. E. Kolb, and M. J. Molina, Chemical kinetics and photochemical data for use in stratospheric modeling: Evaluation 12, *JPL Publ.*, 97-4, 1997.
- Deshler, T., B. J. Johnson, and W. R. Rozier, Balloonborne measurements of Pinatubo aerosol during 1991 and 1992 at 41°N: Vertical profiles, size distribution, and volatility, *Geophys. Res. Lett.*, 20, 1435–1438, 1993.
- Gil, M., O. Puentedura, M. Yela, C. Parrondo, D. B. Jadhav, and B. Thorkelsson, OCIO, NO₂, and O₃ total column observations over Iceland during the winter 1993/94, *Geophys. Res. Lett.*, 23, 3337–3340, 1996.
- Hipler, H., S. Nasterlack, F. Striebel, and D. M. Golden, Reaction OH + NO₂ + M: Proof of isomer formation, poster presented at the Workshop on Nitrogen Oxides in the Lower Stratosphere and Upper Stratosphere, Univ. of Heidelberg, Germany, 19–22 March 2001.
- Knudsen, B. M., J.-P. Pommereau, A. Garnier, M. Nunez-Pinharanda, L. Denis, G. Letrenne, M. Durand, and J. M. Rosen, Comparison of stratospheric air parcel trajectories based on different meteorological analyses, *J. Geophys. Res.*, 106, 3415–3424, 2001.
- Kreher, K., J. G. Keys, P. V. Johnston, U. Platt, and X. Liu, Ground-based measurements of OCIO and HCl in austral spring 1993 at Arrival Heights, Antarctica, *Geophys. Res. Lett.*, 23, 1545–1548, 1996.
- Larsen, N., B. Knudsen, J. Rosen, N. Kjome, R. Neuber, and E. Kyrö, Temperature histories in liquid and solid polar stratospheric cloud formation, *J. Geophys. Res.*, 102, 23,505–23,517, 1997.
- Lary, D., R. Toumi, A. M. Lee, M. J. Newchurch, M. Pirre, and J. B. Renard, Carbon aerosols and atmospheric photochemistry, *J. Geophys. Res.*, 102, 3671–3682, 1997.
- Lefèvre, F., F. Figarol, K. S. Carslaw, and T. Peter, The 1997 Arctic ozone depletion quantified from three-dimensional model simulations, *Geophys. Res. Lett.*, 25, 2425–2428, 1998.
- Madronich, S., and S. Flocke, The role of solar radiation in atmospheric chemistry, in *Handbook of Environmental Chemistry*, edited by P. Boule, pp. 1–26, Springer-Verlag, New York, 1999.
- McNally, A. P., E. Andersen, G. Kelly, and R. W. Saunders, The use of raw TOVS/ATOVS radiances in the ECMWF 4D-Var assimilation system, *ECMWF Newsl.*, 83, 1999.
- Orlando, J. J., and G. S. Tyndall, Rate coefficients for the thermal decomposition of BrONO₂ and the heat of formation of BrONO₂, *J. Phys. Chem.*, 100, 19,398–19,405, 1996.
- Payan, S., C. Camy-Peyret, P. Jeseck, T. Hawat, M. Pirre, J.-B. Renard, C. Robert, F. Lefèvre, H. Kansawa, and Y. Sasano, Diurnal and nocturnal distribution of stratospheric NO₂ from solar and stellar occultation measurements: Comparison with models and ILAS satellite measurements, *J. Geophys. Res.*, 104, 21,585–21,593, 1999a.
- Payan, S., *et al.*, HALOMAX results on reservoir and active chlorine species: Balloon measurements and comparisons with 3-D chemical transport model, stratospheric ozone 1999, in *Proceedings of the Fifth*

- European Symposium, 27 September to 1 October 1999*, Saint Jean de Luz, France, 1999b.
- Pierson, J. M., K. A. McKinney, D. W. Toohey, J. Margitan, U. Schmidt, A. Engel, and P. A. Newman, An investigation of ClO photochemistry in the chemically perturbed Arctic vortex, *J. Atm. Chem.*, **32**, 61–81, 1999.
- Pommereau, J. P., and J. Piquard, Observation of the vertical distribution of stratospheric OCIO, *Geophys. Res. Lett.*, **21**, 1231–1234, 1994a.
- Pommereau, J. P., and J. Piquard, Ozone, nitrogen dioxide and aerosol vertical distribution by UV-visible solar occultation from balloon, *Geophys. Res. Lett.*, **21**, 1227–1230, 1994b.
- Renard, J. B., M. Pirre, C. Robert, G. Moreau, D. Huguenin, and J. M. Russell III, Nocturnal vertical distribution of stratospheric O₃, NO₂ and NO₃ from balloon measurements, *J. Geophys. Res.*, **101**, 28,793–28,804, 1996.
- Renard, J. B., F. Lefèvre, M. Pirre, C. Robert, and D. Huguenin, Vertical profile of night-time stratospheric OCIO, *J. Atmos. Chem.*, **26**, 65–76, 1997.
- Renard, J. B., M. Pirre, and C. Robert, the possible detection of OBrO in the stratosphere, *J. Geophys. Res.*, **103**, 25,383–25,395, 1998.
- Renard, J. B., M. Chartier, C. Robert, G. Chalumeau, G. Berthet, M. Pirre, J. P. Pommereau, and F. Goutail, SALOMON: A new, light balloonborne UV-visible spectrometer for nighttime observations of stratospheric trace-gas species, *Appl. Opt.*, **39**, 386–392, 2000.
- Rivière, E. D., et al., Role of lee waves in the formation of solid polar stratospheric clouds: Case studies from February 1997, *J. Geophys. Res.*, **105**, 6845–6853, 2000.
- Roche, A. E., J. B. Kumer, J. L. Mergenthaler, G. A. Ely, W. G. Uplinger, J. F. Potter, T. C. James, and L. W. Sterritt, The Cryogenic Limb Array Etalon Spectrometer (CLAES) on UARS: Experiment description and performance, *J. Geophys. Res.*, **98**, 10,763–10,775, 1993.
- Saathoff, H., K.-H. Naumann, N. Riemer, S. Kamm, O. Möhler, U. Schurath, H. Vogel, and B. Vogel, The loss of NO₂, HNO₃, NO₃/N₂O₅, and H₂O/HOONO₂ on soot aerosol: A chamber and modeling study, *Geophys. Res. Lett.*, **28**, 1957–1960, 2001.
- Sander, S. P., et al., Chemical kinetics and photochemical data for use in stratospheric modeling, supplement to evaluation 12: Update of key reactions, evaluation number 13, *JPL Publ.*, 0-3, 2000.
- Sanders, R. W., S. Solomon, K. Kreher, and P. V. Johnston, An intercomparison of NO₂ and OCIO Measurements at Arrival Heights, Antarctica during Austral Spring 1996, *J. Atmos. Chem.*, **33**, 283–298, 1999.
- Schiller, C., and A. Wahner, Comment on “Stratospheric OCIO measurements as a poor quantitative indicator of Chlorine activation” by J. Sessler et al., *Geophys. Res. Lett.*, **23**, 1053–1054, 1996.
- Schiller, C., A. Wahner, U. Platt, H.-P. Dorn, J. Callies, and D. H. Ehhalt, Near UV atmospheric absorption measurements of column abundances during Airborne Arctic Stratospheric Expedition, January–February 1989, 2, OCIO observations, *Geophys. Res. Lett.*, **17**, 501–504, 1990.
- Sessler, J., M. P. Chipperfield, J. A. Pyle, and R. Toumi, Stratospheric OCIO measurements as a poor quantitative indicator of chlorine activation, *Geophys. Res. Lett.*, **22**, 687–690, 1995.
- Solomon, P., J. Barrett, B. Connor, S. Zoonematkermani, A. Parrish, A. Lee, J. Pyle, and M. Chipperfield, Seasonal observation of chlorine monoxide in the stratosphere over Antarctica during the 1996–1998 ozone holes and comparison with the SLIMCAT three-dimensional model, *J. Geophys. Res.*, **105**, 28,979–29,001, 2000.
- Solomon, S., G. H. Mount, R. W. Sanders, R. O. Jakoubek, and A. L. Schmeltekopf, Observations of the night time abundance of OCIO in the winter stratosphere above Thule, Greenland, *Science*, **242**, 550–555, 1988.
- van den Broek, M. M. P., A. Bregman, and J. Lelieveld, Model study of stratospheric chlorine activation and ozone loss during the 1996/1997 winter, *J. Geophys. Res.*, **105**, 28,961–28,977, 2000.
- Wetzel, G., H. Oelhaf, T. von Clarmann, H. Fischer, F. Friedl-Vallon, G. Maucher, M. Seefeldner, O. Trieschmann, and F. Lefèvre, Vertical profiles of N₂O₅, HO₂NO₂, and NO₂ inside the Arctic Vortex, retrieved from nocturnal MIPAS-B2 infrared limb emission measurements in February 1995, *J. Geophys. Res.*, **102**, 19,177–19,186, 1997.

G. Berthet, M. Chartier, N. Huret, M. Pirre, J.-B. Renard, and E. Rivière, Laboratoire de Physique et Chimie de l'Environnement, 3A, Avenue de la Recherche Scientifique, F-45071 Orléans cedex 02, France. (riviere@cnsr-orleans.fr; mpirre@cnsr-orleans.fr; gberthet@cnsr-orleans.fr; jbreward@cnsr-orleans.fr; nhuret@cnsr-orleans.fr)

B. Knudsen, Danish Meteorological Institute, Lyngbyvej 100, Denmark. (bk@DMI.dk)

F. Lefèvre, Service d'Aéronomie du CNRS/IPSL, Université Pierre et Marie Curie, 4 place Jussieu, BP 102, F-75252 Paris cedex 05, France. (franck.lefevre@aero.jussieu.fr)